Observations of the Coastal Upwelling Region near 34°30'N off California: Spring 1981[1]

KENNETH H. BRINK

Woods Hole Oceanographic Institution, Woods Hole, MA 02543

DAVID W. STUART

Department of Meteorology, Florida State University, Tallahassee, FL 32306

JOHN C. VAN LEER

Rosenstiel School of Marine and Atmospheric Sciences, University of Miami, Miami, FL 33149

(Manuscript received 31 January 1983, in final form 8 November 1983)

ABSTRACT

Coordinated meteorological and oceanographic (CTD) measurements were made near Point Conception, California, during March–April 1981. The goal of the observations was to study coastal upwelling and the local characteristics of the assumed wind driving. Results showed substantial topographically-induced spatial structure in the near-surface winds, with weaker winds generally occurring within the Santa Barbara Channel. The 1981 "spring transition" event was monitored by means of hydrographic and sea level measurements. The details of the event suggest that it was not entirely driven by local wind stress. The mean sea surface temperature pattern suggests the existence of an upwelling center between Points Arguello and Conception. The individual sea surface temperature charts are all dominated by patchiness on a scale of 5–15 km. The nature of these structures is not well understood, but on the one occasion when a patch was isolated by a CTD survey, its structure penetrated to at least 50 db.

1. Introduction

The 1976–77 observations taken off the coast of Peru near 15°S during the CUEA (Coastal Upwelling Ecosystem Analysis) program demonstrated the existence of a coastal upwelling center ("plume") at that location. The results (e.g., Brink *et al.*, 1981; Stuart, 1981; Boyd and Smith, 1982) showed that the structure was highly time-variable and that its strength and size were strongly dependent upon the local winds. Further, the structure was often clearly associated with complementary structures in biological fields. The Peru study left unanswered numerous questions about the flow and hydrographic fields associated with the structure. Interdisciplinary interest in the further study of upwelling centers eventually led to the establishment of the OPUS (Organization of Persistent Upwelling Structures) program.

The OPUS program sought to locate and to study an upwelling structure off the west coast of the United States that could be compared to that off Peru. A candidate area was found in the region near Points Arguello and Conception (near 34°30'N) off southern California. The location has been known to be a locale of strong coastal upwelling from the time of the pioneering study of Sverdrup (1938). Since then, studies such as that of Reid (1965) have confirmed the existence of upwelling at that location. Satellite observation of surface temperature (e.g., Breaker and Gilliland, 1981) reinforced the impression of localized strong upwelling in the Arguello–Conception area.

The OPUS pilot program was undertaken during spring 1981 as preparation for a potential future experiment. The primary goal of the observations was to gain some knowledge of the space and time scales of the meteorological and oceanographic systems. The findings of the pilot program were, however, of interest more than simply as design parameters. For example, the results include an unusually temporally-intensive hydrographic dataset documenting a west coast "spring transition" event (e.g., Huyer *et al.*, 1979). In the following, we will summarize some of the more salient results of the pilot program, without attempting to be exhaustive. First we will discuss the behavior of the atmospheric forcing, then the hydrographic temporal variability and finally the three-dimensional structure of the system.

2. Observations

The OPUS pilot experiment took place from 4 March–15 April 1981, in the region centered on Points

[1] Woods Hole Oceanographic Institution Contribution No. 5319.

Arguello and Conception, California (near 34°30'N). The time of year was chosen to coincide with the climatological onset of the strong local coastal-upwelling season (e.g., Hickey, 1979). The measurements reported here fall into two general categories: meteorological and physical oceanographic. A description of the overall interdisciplinary dataset is given by Jones *et al.* (1983).

a. Meteorological

Surface (10 m) winds, air pressure and air and water temperatures were obtained on an hourly basis throughout the observation period from the NOAA buoy (NDBO 46011) located at 34°53'N, 120°52'W, about 20 km offshore of Point Sal and about 35 km north of Point Arguello (Fig. 1). This over-the-water record was taken to be the standard OPUS wind time series. Wind stress was computed using the formulas of Large and Pond (1981) and then low-pass filtered using the Oregon State University LLPA (half-power point at 1.96 days) filter. In addition, shorter (18–31 March) wind records were obtained from temporary, analog-recording anemometers at Purisima Point (Pt. P) and near Point Conception (C-5 and C-8, see Fig. 1). Finally, weather maps and other measurements of larger-scale atmospheric patterns were collected and analyzed.

Aircraft measurements were made using the NCAR Queenair. All flights were made during a 3–4 hour period centered at noon local time. Sea surface temperature (SST) data were obtained with a Barnes PRT-5 radiometer having a 2° field of view, sensing in the spectral region of 9.5–11.5 microns. Aircraft position was obtained by an inertial navigation system (LTN-51 by Litton) and altitude (152 m) was determined by a radio altimeter. Each flight provided wind velocity and sea surface temperature data, which were mapped using values sampled each minute, or every 4.6 km. The winds represent 30-second averages, while the temperature points are, at most, 3-second averages. Individual maps were discretized onto a grid 2′ of latitude by 3′ of longitude to facilitate temporal averaging. At the end of each flight, an aircraft sounding was made from 15 to 1829 m elevation, at a location roughly 35 km farther offshore than the NOAA buoy (Fig. 1). Each sounding included measurements of winds, air temperature, dew point temperature and atmospheric pressure. Ten mapping flights were conducted during 18–31 March, seven of which (18, 20, 22, 28, 29, 30 and 31 March) covered the region between Points Arguello and Conception. Further details are given by Stuart and Linn (1983).

b. Oceanographic

The primary dataset consists of CTD measurements made during three legs aboard the R.V. *Velero IV* during 4 March–15 April 1981. The system used was a Plessy 9040, as described by Limeburner and Beardsley (1979). Further, LLPA (see above) filtered records of adjusted (sea level plus atmospheric pressure) sea level from Port San Luis (35°11'N, 120°45'W, ~65 km north of Point Arguello), Rincon Island (34°21'N, 119°26'W, ~95 km east of Point Conception) and Santa Monica (34°01'N, 118°29'W, near Los Angeles) were made available to us, courtesy of Dr. J. S. Allen.

3. The atmospheric setting

The primary goal of the meteorological observations was to characterize the space and time scales of the local wind driving and to provide time series records for use in the interpretation of the oceanographic data.

a. Basic wind record

The standard time series of local alongshore wind stress (Fig. 2) was derived from the NOAA buoy. The alongshore direction (50° counterclockwise from due north) was defined by the locus of Points Arguello and Conception, but it is also comparable to the principal axis direction of the wind, ~35°. The mean winds were clearly equatorward (upwelling favorable) over the period of the OPUS pilot program. The dominant fluctuations in the filtered wind stress record are a series of 3–4 day period oscillations which are associated with the passages of atmospheric highs, lows and associated fronts moving from the west or northwest across the region. These fluctuations correspond to a very clear peak for periods of 2–4 days in the variance-conserving spectrum of scalar winds (Fig. 3). During March, the frontal systems moved eastward rather quickly, yielding short periods of reduced southward or even northward airflow ahead of the cold fronts followed by stronger southward airflow behind the fronts. Shallow cold highs also contributed to the strong southward flow being short-lived. During April, the frontal systems moved through the OPUS region more slowly, generally moving in from the north or northwest. This caused weak southward flow ahead of the fronts and stronger southward flow behind the fronts as the highs built. With generally weaker eastward flow in April, the highs remained in the Arguello–Conception area longer. Also, with heating over the deserts of the Southwest United States, the thermal low over the land strengthened, generally helping to increase the pressure gradient supporting southward flow along the California coast. At times, this thermal low expanded in area or moved enough for the OPUS coastal region to experience a weaker pressure gradient. The major wind fluctuations during March–April 1981 were clearly in response to the surface pressure features as seen on the National Weather Service synoptic-scale maps.

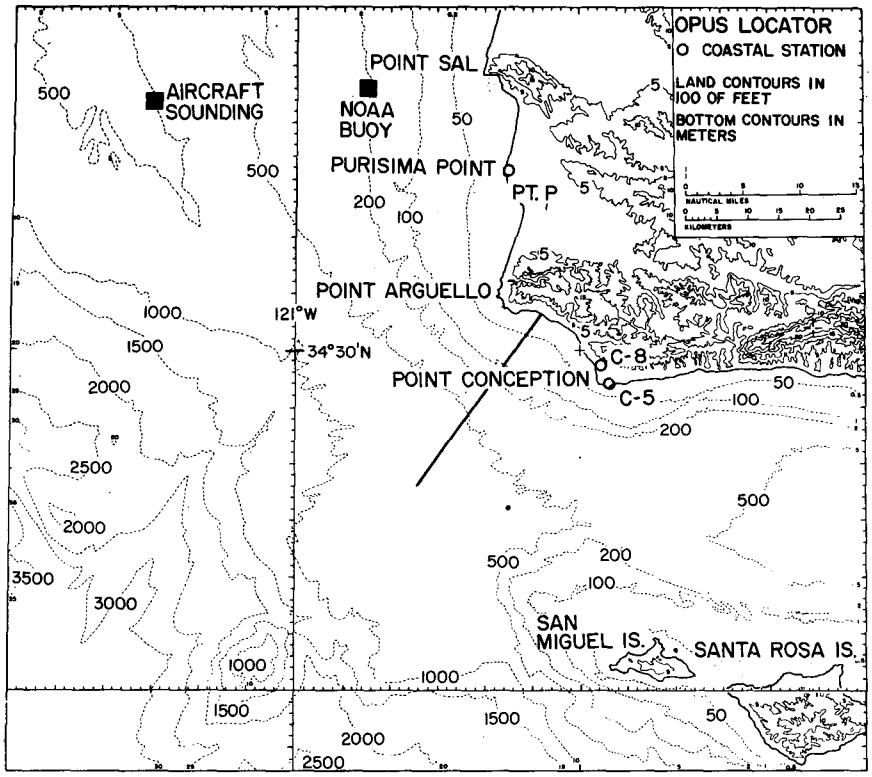

FIG. 1. Locator map of the OPUS area. Water depths are in meters; land elevations are in feet. The bold line running southwest–northeast is the main hydrographic line, the "G-line".

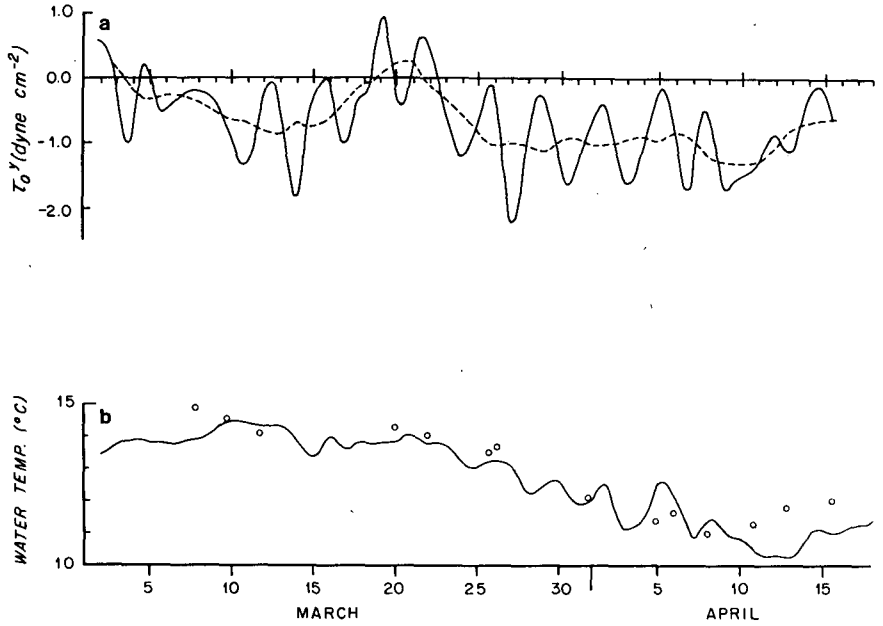

FIG. 2. Low-pass filtered time series from the NOAA buoy. (a) Alongshore wind stress τ_0^y. Positive values correspond to northwestward winds. The dashed line is a four-day running mean, used to accentuate the lower-frequency trends. (b) Sea surface temperature. Circles are surface temperatures observed by CTD at comparable (~20 km) distances from the coast, but closer to Points Arguello and Conception (generally along the G-line).

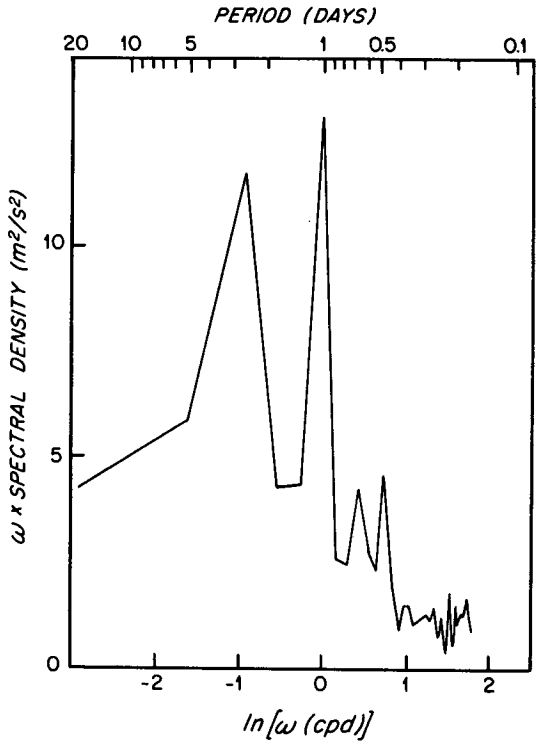

FIG. 3. Variance-conserving autospectrum of scalar winds at the NOAA buoy.

b. Spatial structure in surface winds

The representativeness of coastal wind records has often been a serious concern in the study of air–sea interaction over the continental shelf. The three short-term OPUS anemometers (Fig. 1) at Point P, C-5 and C-8 were compared with the offshore NOAA buoy to address this problem.

As might be expected, the winds over the water were noticeably stronger than those at the coast (Table 1). The wind directions at the NOAA buoy and at Point P were similar at all times. The C-8 wind directions were similar to the buoy winds during periods of generally southward airflow, but during northward flow, the C-8 record tended to show flow more toward the northwest. The C-5 position, just east of Point Conception, tended to have a persistent directional offset relative to the offshore winds. When the airflow at the buoy was southward or southeastward, C-5 tended to have eastward flow. When the flow offshore was northward, C-5 tended to have westward, or slightly south-of-westward flow.

Comparison of the vector wind records can be quantified by use of the complex correlation (e.g., Kundu and Allen, 1976)

$$r_{12} = \frac{1}{N}\sum_{n=1}^{N} \frac{w_1^*(n\Delta t)w_2(n\Delta t)}{[|w_1|^2|w_2|^2]^{1/2}},$$

where

$$w_j = u_j' + iv_j',$$

$i = (-1)^{1/2}$, q^* is the complex conjugate of q and a prime denotes deviation from the time mean. The absolute value of $|r_{12}|$ is a measure of the degree of correlation of the two vector series, independent of orientation. The phase of r_{12} represents the directional offset (positive for w_1 toward the right of w_2) between the vectors at the two positions. Thus, the results of this calculation are independent of the choice of the coordinate system, as long as both records in a pair are in the same orientation. Results of these calculations, using hourly values, are shown in Table 1, and they tend to confirm the more qualitative descriptions above. The buoy wind fluctuations are well correlated with those at all other positions ($|r_{12}| \geq 0.73$), but the directional offset relative to buoy winds is clearly greatest at C-5. Hence, considerable caution must be taken in the use of coastal wind records for comparison with oceanographic measurements, a finding that may well have been anticipated based on past experience.

c. Spatial patterns in 152 m winds

The horizontal structure of the wind field is more thoroughly addressed through the aircraft wind maps. First, however, some attention must be paid to the representativeness of the flight-level (152 m) winds relative to the near-surface (10 m) buoy winds.

Aircraft soundings made offshore of the NOAA buoy showed that the lapse rate was within error (±0.1°C km^{-1}) of the adiabatic up to the flight level in six of the seven relevant cases. Furthermore, soundings made at Vandenberg Air Force Base inshore of Purisima Point about two hours after the end of each flight always showed an adiabatic lapse rate up to and above the flight level. In other words, most of the flights were apparently conducted at a sufficiently low level to be within the well-mixed layer. This would suggest that similar processes govern the 10 m and 152 m winds and that their behavior should also be similar.

On each flight the aircraft passed over the NOAA buoy at an altitude of 152 m. Using buoy wind data for the nearest reporting hour (i.e., ±30 min of actual overflight time), the wind components at the buoy and at the aircraft were compared (Table 2). For this com-

TABLE 1. Complex correlations between hourly wind time series (18–31 March 1981).

Record	$\bar{u}$ (m s^{-1})	$\bar{v}$ (m s^{-1})	$\overline{\lvert v'\rvert^2}^*$ (m^2 s^{-2})	$\lvert r_{12}\rvert$†	θ
NOAA	3.26	−2.67	37.6	—	—
Point P	1.36	−2.21	22.2	0.84	−2°
C-5	2.91	0.21	20.4	0.75	+72°
C-8	1.38	−2.01	14.5	0.73	+14°

* $\frac{1}{N}\sum(u'^2 + v'^2)$.

† Series 1 is always the NOAA buoy wind record.

TABLE 2. Regression fits between near-surface and 152 m winds. $[(u, v)|_{\text{lower}} = a + b(u, v)|_{152\text{ m}}]$.

	a (m s^{-1})	Error in a (m s^{-1})	b	Error in b	Correlation
Buoy (10 m) winds vs 152 m					
u (E–W)	0.82	1.00	0.77	0.16	0.86
v (N–S)	−0.19	0.80	0.78	0.09	0.95
Aircraft 15 m winds vs 152 m					
u (E–W)	1.90	1.2	0.60	0.18	0.77
v (N–S)	0.03	0.40	0.89	0.05	0.99

parison only, it is convenient to break from convention and use a geographical coordinate system. The more energetic v winds (N–S) were very well correlated between the levels, but the u winds (E–W) less so. Regression fits, however were very similar for both components. Using the wind data from only the aircraft soundings, the 15 m winds were also compared to the 152 m winds. In this case, the winds at both levels were measured within 1–2 minutes of each other. Correlations between levels were again rather good, especially for the v (N–S) component (Table 2), but the mean offset a for the u (E–W) component was not within error of zero. Directional offsets between levels were small (<5°), with flight level winds tending to be slightly toward the left of lower level winds.

From the preceding, we conclude that the aircraft (152 m) results yield a useful synoptic mapping of surface winds over the study region. However, the amplitudes of the near-surface winds appear to be about 0.6–0.9 of those at flight level. Although the patterns in aircraft-estimated 10 m winds are reliable, the quantitative relation (Table 2) has large enough error bars to make estimates of derived quantities (such as 10 m wind stress curl) unreliable.

As a means of simplifying the presentation of the wind observations, we have chosen to present only maps of winds averaged by general airflow direction. Specifically, Fig. 4a shows the average noontime 152 m velocity of 18 and 20 March 1981, when the airflow was predominantly northward, and Fig. 4b depicts airflow averaged over 22, 28, 29, 30 and 31 March, when the flow was generally toward the south. These averaged maps, while not very meaningful statistically, are repeatable in their major features and thus, can be taken as representative. Furthermore, they clearly contrast the predominant northward and southward airflow regimes.

The mean winds during the northward regime (Fig. 4a) show northeastward flow in the southwestern section of the region, but airflow becomes mainly northward to the west and north of Point Arguello. A local veering associated with the Channel Islands is clearly visible near the southeastern corner of the mapping region. The wind speeds are generally low (<3 m s^{-1}) over most of the region east and directly south of Point Arguello, but to the west, speeds generally increase to 4–8 m s^{-1}. The structure of the 7 and 8 m s^{-1} isotachs near Point Sal is probably in part orographically induced. The two individual flights used for this mean map are both similar to the mean, particularly regarding the weak winds south of Points Arguello and Conception and into the Santa Barbara Channel. Both individual charts have zonally oriented isotachs north of Point Arguello, but the 18 March flight had a particularly strong wind maximum 10–15 km offshore between Points Sal and Arguello.

The mean map from the southward regime (Fig. 4b) shows airflow generally toward the southeast with slightly eastward veering near the coast, especially to the east of Point Conception. The strongest winds (greater than 10 m s^{-1}) were just south of Point Arguello and directly south of Point Conception. Wind speeds as low as 6 m s^{-1} were found near the coast to the north of Point Arguello and between Points Arguello and Conception. The isotachs were oriented roughly north–south across the western end of the Santa Barbara Channel, corresponding to much weaker winds to the east.

Since data from five flights were used in Fig. 4b, some comments on the individual maps are in order. In all five cases, the streamline patterns to the north and west of Point Conception are quite similar to those in the mean map. Nearly all the cases showed a narrow coastal band of weak winds to the north of Point Arguello and near the coast between Points Arguello and Conception. Most cases showed double wind speed maxima associated with the Points, but not always in the same places and generally not of equal magnitude. On some flights, e.g., 29, 30 and 31 March, when the overall southeastward flow was moderately strong, the airflow took on a more eastward component just east of Point Conception. On 29 March, the flow veered again toward the southeast farther into the Channel, but on 31 March, the eastward flow persisted well to the east of Point Conception. However, on 30 March, a day of strong southward flow (Fig. 2), the airflow direction showed little deviation near Point Conception. Generally, when the overall wind was strongest, the wind direction and speed were less affected by Point Conception, while when overall winds were weaker, more eastward airflow was observed east of Point Conception and the wind strength dropped off quickly to the east.

Some caution must be taken in the interpretation of the aircraft maps because of possible temporal aliasing. For example, the east–west (dominant direction) component amplitude of the sea breeze was 1.9 and 2.3 m s^{-1} at the NOAA buoy and at Point P respectively. The wind maps were, however, made at ~1200 local time, when the sea breeze components were relatively weak. Thus, we have some confidence in the temporal representativeness of the aircraft wind measurements.

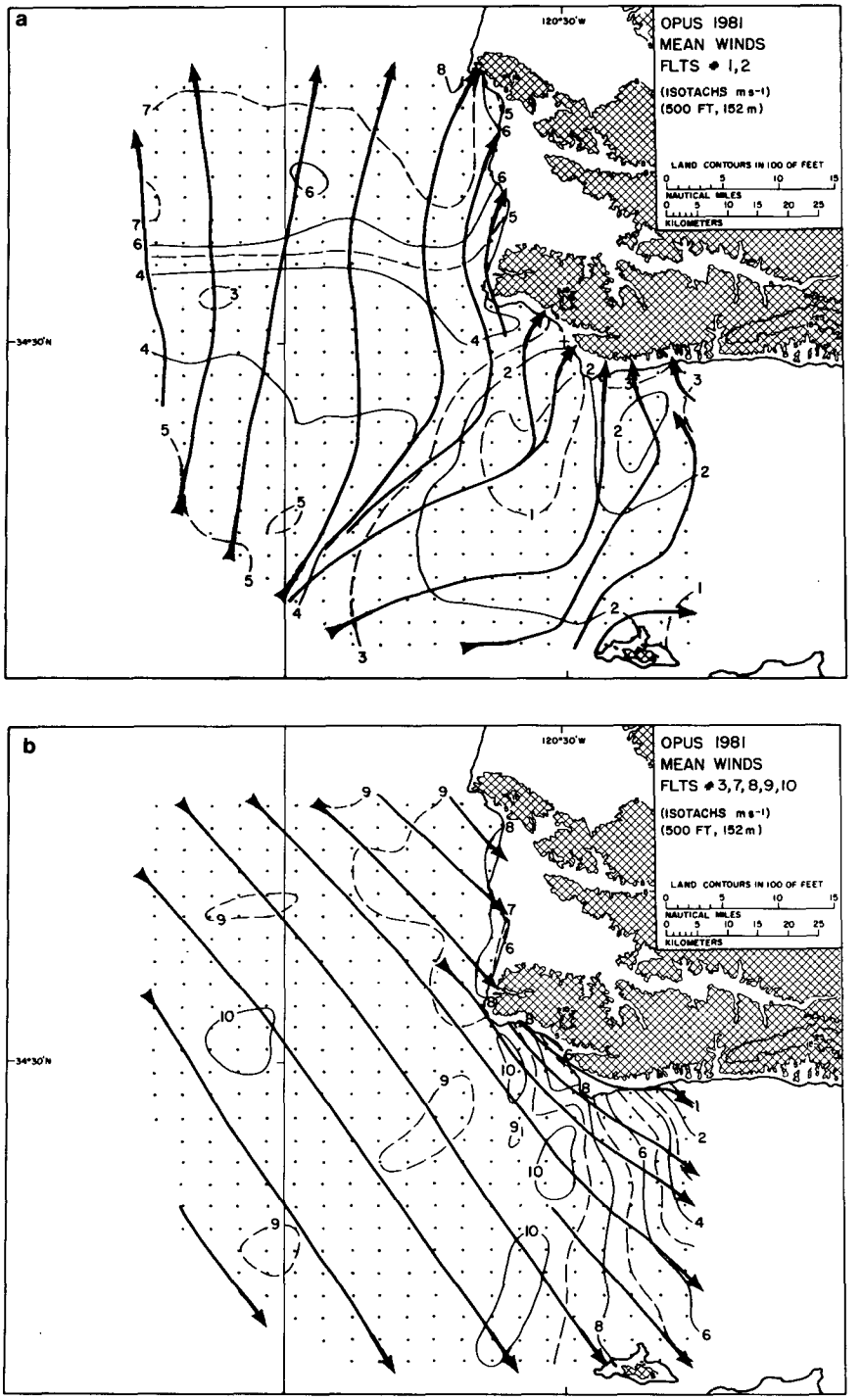

FIG. 4. Mean 152 m winds derived from aircraft overflights. Heavy lines (streamlines) give wind directions and lighter contours are isotachs in m s^{-1}. Land higher than 152 m (500 ft) above sea level has been cross-hatched. Dots are the digitization grid used for averaging: (a) generally northward airflow (18 and 20 March 1981) and (b) generally southward airflow (22, 28, 29, 30 and 31 March 1981).

The results of the wind mapping program suggest that there was generally substantial horizontal structure in the strength of the wind field, manifested in both a wind shadow in the Santa Barbara Channel during southward winds and in occasional acceleration effects close to the headlands. These effects will be further accentuated in the wind stress field. The dramatic differences between the C-5 and C-8 coastal winds, for

example, can perhaps be better understood in light of these overall patterns.

4. Oceanic aspects

The observed oceanic system proved to be strongly three-dimensional and dramatically time-dependent. To discuss the system's behavior in an orderly way, we will split the discussion first by treating the time dependence in a roughly two-dimensional manner and then by treating three-dimensional aspects at particular times. This approach is reasonable in light of the relative sparseness of synoptic data giving resolution in horizontal planes.

a. Time dependence

Perhaps the clearest way to appreciate the time dependence of the system is to consider the CTD sections of density from 11 and 31 March and 7 and 12 April (Fig. 5) in light of the alongshore wind stress from the NOAA buoy (Fig. 2). Only density (σ_t) is shown, since

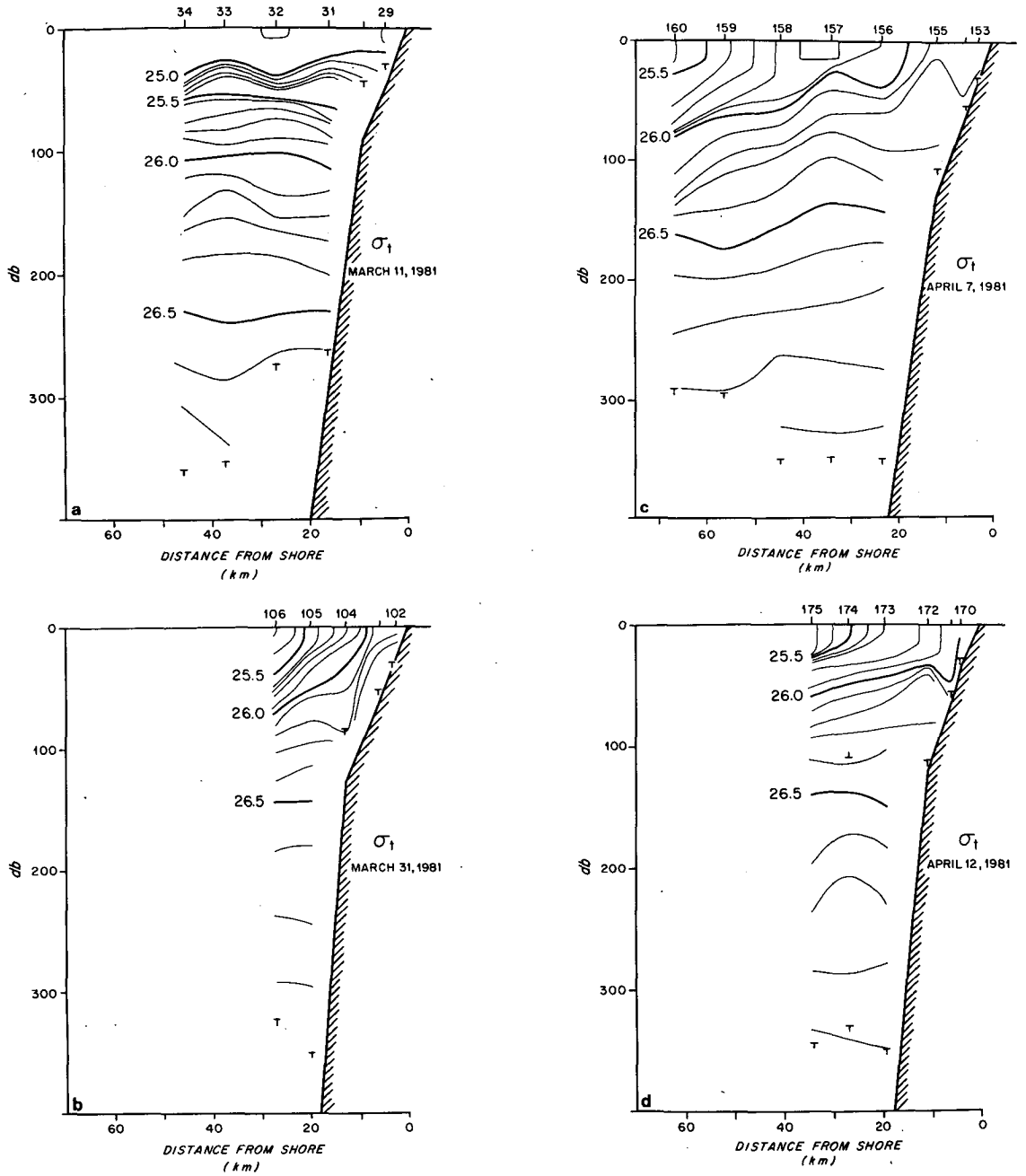

FIG. 5. Density sections normal to the coast between Points Arguello and Conception for (a) 11 March, (b) 31 March, (c) 7 April and (d) 12 April 1981.

T–S diagrams tend to have a nearly linear structure over approximately the upper 200 db so that nearly equivalent information is obtained from temperature, salinity or density in this range. All density sections shown were taken roughly normal to the coast, originating within ~3 km of the halfway mark between Points Arguello and Conception (Fig. 1). Over the period of 7 March–15 April 1981 23 CTD sections were made in the overall region; these four particular sections were chosen as representative. Some of the sections not shown have more structure on scales of 5–10 km, especially within roughly the upper 100 db of the water column.

During the initial period of 7 March until about 21 March, a distinct pycnocline was generally present at ~50–100 db pressure, which could be associated with roughly the 25.5σ_t-surface (Fig. 5a). Although the alongshore wind stress tended to be southeastward (negative) throughout this period, dramatic signs of coastal upwelling (e.g., fronts) were absent, and surface temperatures observed by CTD never went below 13°C, nor surface density above 25.2. However, there appeared to be strong suggestions of nearly monotonically upward motions, as suggested by the depths of σ_t-surfaces at, for example, 20 km offshore (Fig. 6).

The onset of an extended period of continuously upwelling favorable winds (Fig. 2) started 23 March, which also marked the beginning of a gradual emergence of a distinct upwelling front. We describe "front" to mean the surface outcropping of the pycnocline and the consequent relatively intense horizontal density gradient at the surface. By 31 March (Fig. 5b), the front had fully emerged with the near shore outcropping of the 26.1 (~10.0°C) σ_t-surface. Initially, this surface had been at approximately 130 db, leading to a gross estimate of vertical velocity of ~5 m d^{-1} up to this point. The front, which should be associated with the surface 25.1–26.0 isopycnals, is not fully resolved in Fig. 5b. The along-frontal surface velocity (estimated geostrophically relative to 330 db) was ~45 cm s^{-1} in the equatorward (southeastward) direction. Nearly all of the shear existed in the upper 100 db of the water column.

The emergence of the upwelling front coincided with a dramatic drop in adjusted coastal sea level at Port San Luis (the nearest available tidegage record, roughly 65 km north of Point Arguello) (Fig. 7). Also shown in the figure are values of steric height at the coast relative to 200 db, calculated following Huyer (1980). The drop in sea level tends to coincide with the frontal emergence which in Fig. 7 roughly parallels a drop in steric height. This suggests that the drop in sea level is at least partly steric in origin and thus associated with the offshore removal, as a front, of the strong pycnocline. A comparable drop in coastal sea level also occurred within 0.5 days at Rincon Island (in the eastern end of the Santa Barbara Channel) and about two days later at Santa Monica, near Los Angeles. Further, Allen (personal communication, 1983) has

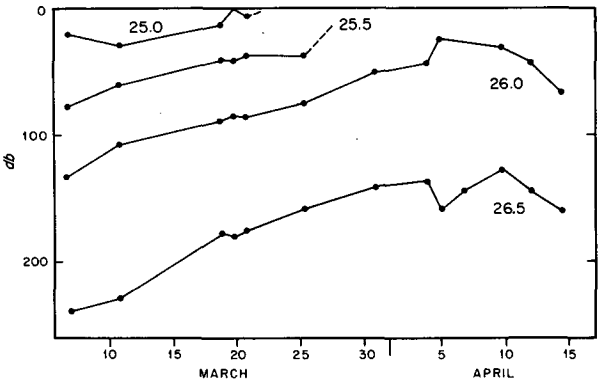

FIG. 6. Depth of selected σ_t surfaces versus time, 20 km from shore between Points Arguello and Conception.

gathered evidence that this dramatic sea level drop occurred all along the United States west coast at roughly the same time. Comparison of Figs. 6 and 7 shows that the sea level drop (density increase) occurred while the apparent vertical velocity was roughly uniform. That is, the sea level drop apparently did not coincide with a surge in vertical velocity. This interpretation is consistent if one pictures the uniform advection of a strong pycnocline past a fixed point.

After the front surfaced, it moved offshore and became much more diffuse with time. The maximum offshore excursion of the frontal center, defined by the 25.5σ_t-surface, appeared to be ~60 km around 7 April (Fig. 5c). Inshore of the frontal boundary, the stratification had become rather weak, and no water denser than 26.2 was observed at the surface. The trend of rising isopycnal surfaces weakened somewhat over this period (Fig. 6).

By 10 April, the 25.5 isopycnal at the sea surface appeared to begin a return migration toward the coast, a tendency that continued until the end of the observations on 15 April (Fig. 5d). Also, the pycnocline became more evident at the offshore end of the sections, e.g., the 25.3–26.0σ_t-surfaces at station 175 in Fig. 5d. During this period, isopycnal surfaces began to subside, and the San Luis sea level showed a clear rising trend (Figs. 6 and 7). This occurred despite the wind remaining favorable for upwelling throughout the observations and, in fact, showing a maximum of smoothed winds about 10 April (Fig. 2). If the upwelling frontal location were determined only by the offshore wind-driven Ekman transport, the front or position of the 25.5 isopycnal, should have still been migrating offshore, and the vertical-velocity component should have been upward at the end of the observation period. This strongly suggests that the upwelling dynamics was not entirely tied to the local winds.

The CTD data, while very useful for showing general characteristics of the ocean's response, have some shortcomings. First, the data were sampled only sporadically in time (see the dots in Fig. 7). This allowed the distinct possibility of temporal aliasing, a problem

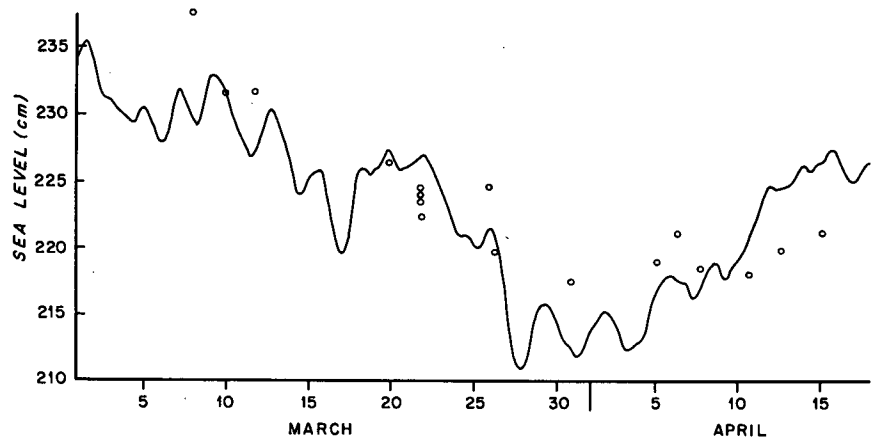

FIG. 7. Low-pass filtered (LLPA) corrected sea level at Port San Luis. Circles represent coastal steric height, extrapolated by Huyer (1980). Multiple circles occur on 21 March and 15 April, days of several-line CTD surveys.

that is particularly acute for the question of the response of the ocean to the dominating 3–4 day oscillations in wind stress (Fig. 3). A second difficulty with the section data is that they represent only a two-dimensional slice through a strongly three-dimensional system. Thus, the offshore distance of the upwelling front along a given section may not be a very fair representation of the system when eddies and frontal meandering are considered.

To fill in the gaps in the time domain, it is useful to study the available continuous records of sea level (San Luis), sea surface temperature (SST) and winds from the NOAA buoy. The adjusted coastal sea level should prove a useful proxy for alongshore currents over the shelf, based on experience with other regions (e.g., Smith, 1974; Brink *et al.*, 1980). This should be true if the alongshore currents are in geostrophic balance and the currents coastally trapped. The San Luis sea level was most coherent with the north–south wind stress component, and significant coherences are found for only the 3.2- and 9-day period bands with the sea level lagging the wind by 0.3–0.6 days. In the broader sense of correlations, the two time series are well correlated, i.e., 0.52 with the wind leading by 0.5 days. These results lend some credence to the idea that the alongshore currents are at least partially wind-driven over time scales shorter than could be resolved by the hydrographic data.

Further evidence for the nature of the ocean's response can be found from the relation between the winds and sea surface temperature at the NOAA buoy. A simple relationship is not necessarily anticipated because of the different ways that SST can be affected by the wind; e.g., mixed-layer deepening (SST decreasing with large wind speeds) and coastal upwelling (SST decreasing only with equatorward winds). The ambiguity is somewhat relieved because the alongshore wind stress is large relative to the across-shelf component (-0.67 versus -0.13 dyn cm^{-2} in the mean and 0.58 versus 0.19 dyn cm^{-2} in standard deviation) and because the alongshore wind stress is generally equatorward during the period considered (Fig. 2). Cross-spectral calculations show that the two time series (τ_0^y, SST) are coherent only at a seven-day period (0.70, 8° ± 21° phase shift). The two series are significantly, but weakly, correlated—0.35 (98% confidence) with τ_0^y leading by 0.75 days. These results suggest that the thermal response of the ocean may not be very great for higher frequency ($\geq$0.2 cpd) fluctuations. Some caution is required, however, since SST measured ~20 km from shore is probably not a very conclusive measure of coastal upwelling.

b. *Spatial structure*

The most comprehensive dataset available for the study of spatial structure is the aircraft-derived maps of sea surface temperature. Seven of these charts were made in the region centered on Points Arguello and Conception during the period of 18–31 March 1981. This period included an initial interval of predominantly northwestward airflow (18–23 March, three charts) and the beginning of the extended period of persistently southeastward airflow (23–31 March, four charts). Recall also that the upwelling front, as defined from CTD results, surfaced during 25–31 March. The first, prefrontal, set of maps showed sea surface temperatures typically in the range of 12–15°C, while the second set showed typical values of 9–14°C. The mean values decreased after frontal emergence, and the ranges of values increased considerably.

The overall mean chart of SST shows what appears to be a fairly well-defined structure (Fig. 8). The lowest values (11.3°C) of mean SST were found just east of Point Arguello, directly against the coast. A second coastal pocket of water nearly as cold was located just north of Point Arguello. Generally, mean SST increased with distance offshore, a trend consistent with

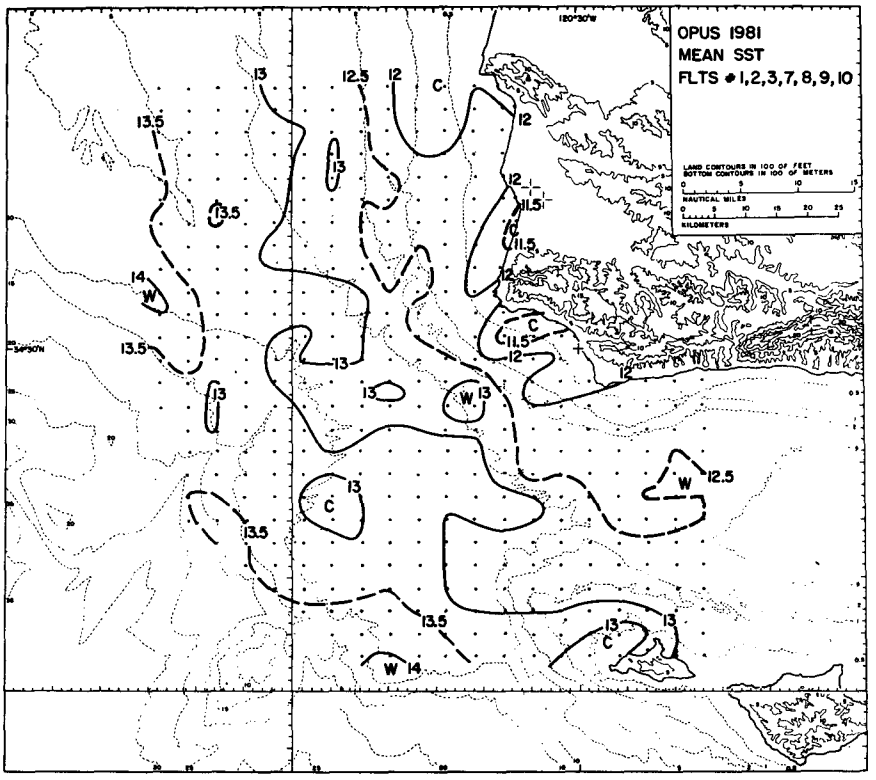

FIG. 8. Mean noontime sea surface temperature (SST) derived from the 152 m aircraft flights of 18, 20, 22, 28, 29, 30 and 31 March 1981.

the presence of coastal upwelling. The mean aircraft SST map tends to confirm the existence of an upwelling center east of Point Arguello, although the structure does not appear to stand out above the background as clearly as that near 15°S off Peru (e.g., Brink *et al.*, 1981).

The mean map shows considerable structure, suggestive of a high degree of variability in the individual charts. Fig. 9 shows two individual realizations of the surface temperature field, one prefrontal (20 March) and one post-frontal (30 March). Both of these charts, as well as all of the others not shown (but see Stuart and Linn, 1983), display structure having spatial scales of 5–15 km and temperature contrasts of ~0.5–2.0°C. These patches are ubiquitous in the sense that they show up to an equal extent on all maps regardless of wind strength or direction. Individual features are highly transitory in that they cannot be unambiguously followed on a day-to-day basis. Because of this, a "drift direction" for the patches cannot be defined. This lack of simplicity is consistent with either drift speeds of ≥ 25 km d^{-1} or with the features being rather short-lived. Some consistency between the individual and mean structures does, however, emerge. For example, individual maps show a tendency for the coldest water to appear near the coast and for warmer water to appear offshore, especially after frontal emergence (Fig. 9b). This is, of course, to be expected from the CTD results.

One of many obvious questions about the SST structure is: how deep does the signature of the patches extend into the water column? Some of the density sections (e.g., Figs. 5a and c) give the impression that the patches are rather superficial features, confined to the upper 10–50 db of the water column. A three-dimensional study of a patch, however, suggests that the structure is more extensive, at least for one realization. The 21 March CTD survey (one of two three-dimensional surveys conducted, Fig. 10) appears to have captured one of these structures rather well. The 3 m temperature chart shows a cold patch occurring off Point Arguello, which was clearly reflected in σ_t at 3 db. Following charts of σ_t to greater depths (Figs. 10c, d and e), it seems fairly clear that there is actually a doming of the isopycnals, with the axis of the feature tilting southeastward with depth at a slope of ~5 m km^{-1}. A comparably dramatic tilt is also found in contour plots of dynamic height anomalies along the various surfaces. The 0–200 db dynamic-height pattern, however, does not coincide with the surface density pattern (e.g., Fig. 10f). In fact, the dynamic height structure appears to be approximately 90–180° out of phase in space relative to the density pattern. If the dynamic height pattern is representative of velocity streamlines, then the overall eddy-associated flow may have tended to advect denser water offshore. This is at least qualitatively consistent with the growth of an unstable disturbance (Pedlosky, 1979) by the eddy removing the mean potential energy associated with

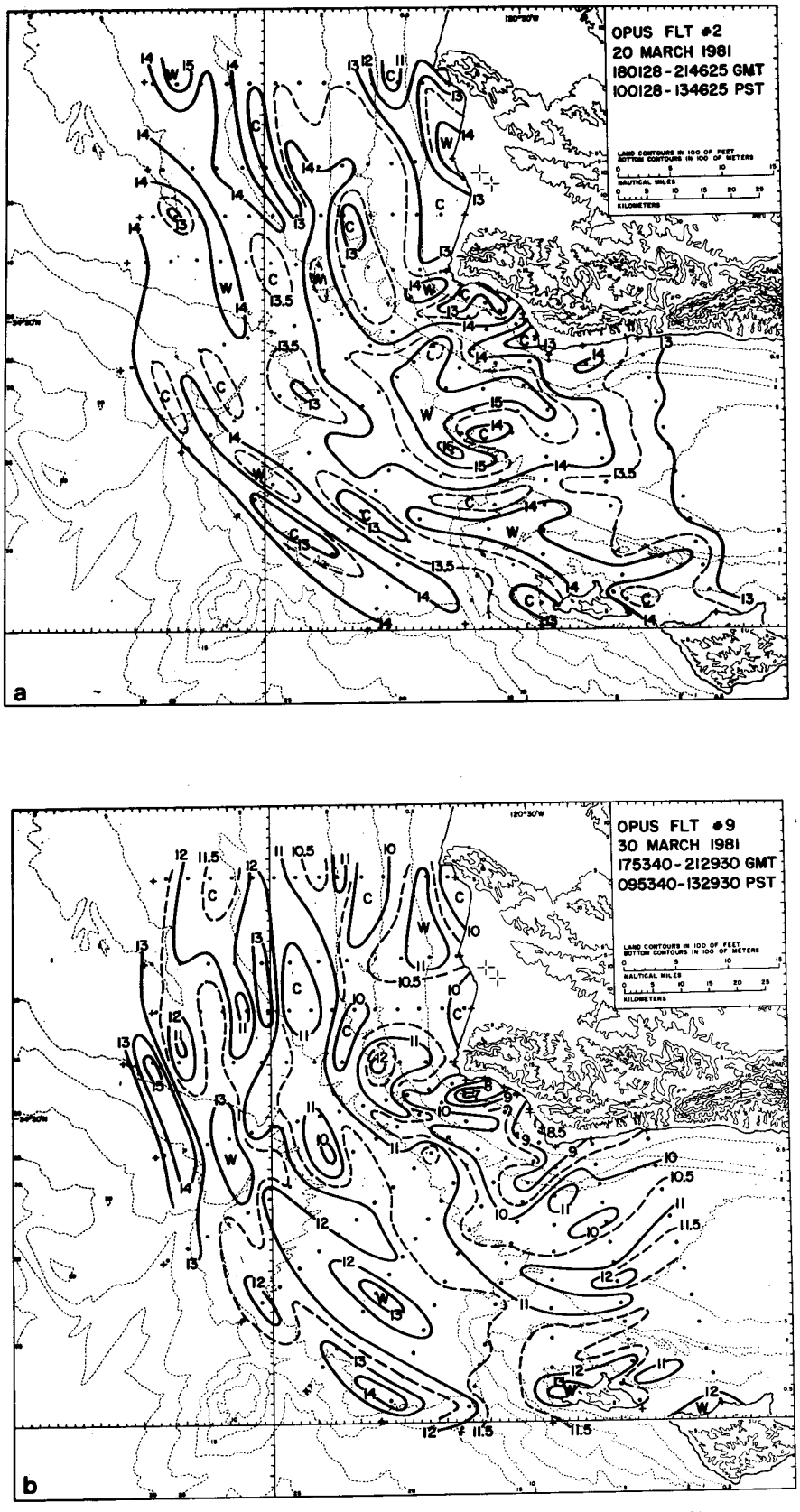

FIG. 9. Noontime sea surface temperature (SST) from individual aircraft overflights for (a) 20 March and (b) 30 March 1981. Dots indicate the flight pattern.

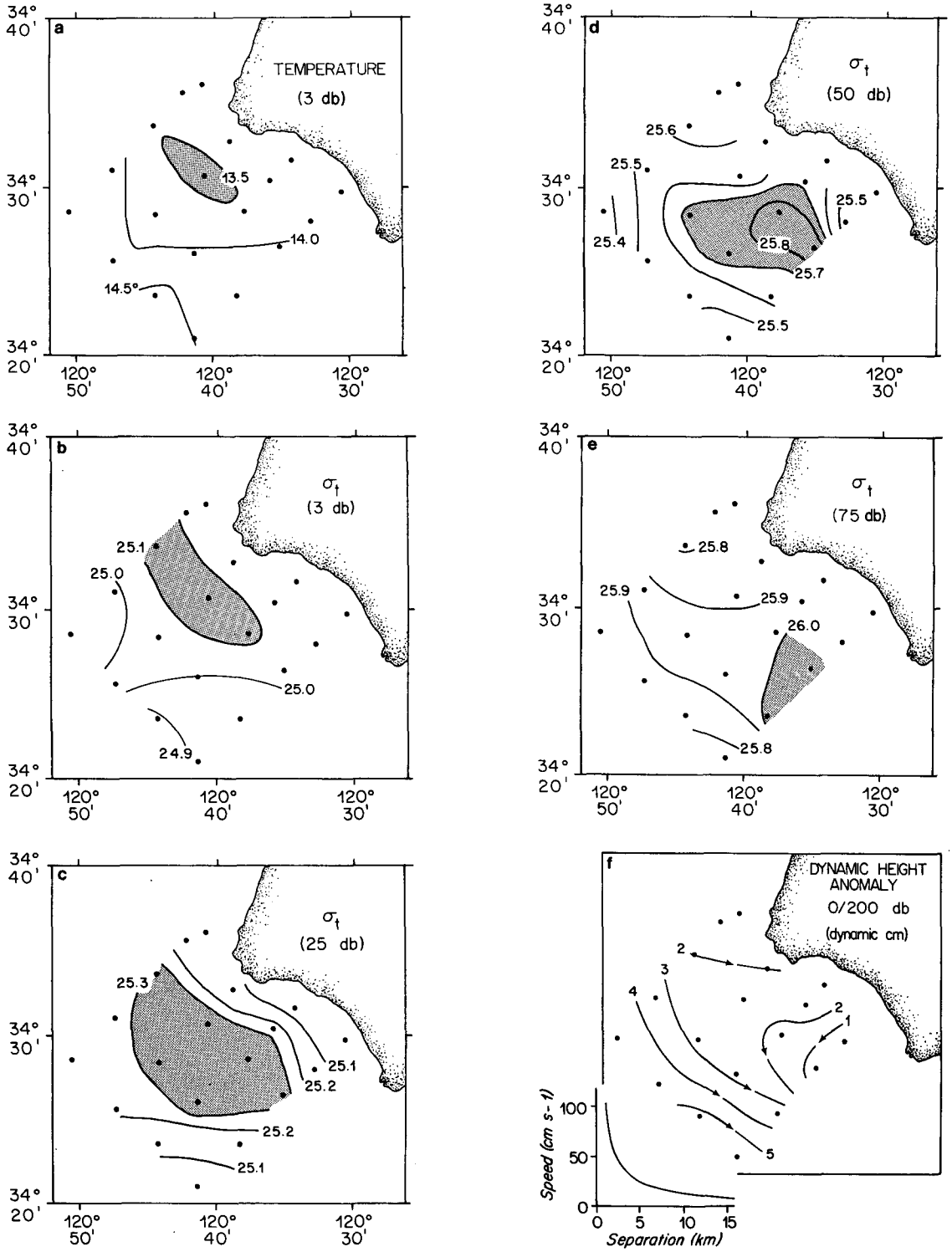

FIG. 10. Results of the 21 March 1981 CTD survey: (a) 3 db temperature (°C), (b) 3 db σ_t, (c) 25 db σ_t, (d) 50 db σ_t, (e) 75 db σ_t and (f) 0–200 db dynamic-height anomaly (dynamic cm). Shallow water values were extrapolated following Huyer (1980). Dots indicate station locations.

mean equatorward flow (i.e., the California Current). This interpretation, however, is fraught with difficulties, primarily because of the problem of obtaining accurate velocity estimates. Further studies in the area, utilizing direct current measurements, would considerably relieve this difficulty.

Given that this particular realization of a "patch" was really a strongly tilting eddy, it seems that the other SST patches may well not be very superficial after all. Individual cross-shelf sections through a tilting eddy would "see" eddy perturbations only over a vertical scale of about 25–50 m (eddy horizontal scale times tilt) and not over the entire depth. Further, an individual section could pass through a portion of the eddy which is entirely subsurface and not show any obvious connection to a surface feature. Thus, deviations of subsurface isopycnals, as in the 12 April section (Figure 5d; 26.6, 26.7σ_t surfaces), may be subsurface reflections of eddies that approach the surface elsewhere.

In conclusion, the system near Points Arguello and Conception is strongly three-dimensional and time-variable. The nature of the dominant (on individual realizations) spatial structures in SST does not appear to be directly associated with the local upwelling process, but perhaps with energetic eddies of indeterminate origin.

5. Discussion

Examination of the dataset reveals two dominating time scales. One is the traditional "event" time scale of 3–10 days, where the ocean appeared to be moderately responsive to local wind fluctuations, but only within well-defined frequency bands (e.g., 3 and 9 day periods for sea level and a 7 day period for surface temperature). The few continuous time series and the available hydrographic data are, however, rather inadequate to form any definitive conclusions on this point. The more dramatic, longer time scale is characterized by a single event (e.g., Figs. 6 and 7) which appears to represent a large-scale spring transition.

Huyer *et al.* (1979) suggested that, off Oregon, an analogous event was triggered by a critical wind event when the amount of time-integrated offshore Ekman transport reached a threshold value. This locally wind-driven interpretation runs somewhat counter to our observations. If the critical event idea were to hold, then the transition would be locally generated in one great surge. One difficulty with this is the vertical velocity which could be inferred from Fig. 6, which suggests a nearly monotonic rising from early March until early April, a period that included substantial poleward wind stresses (Fig. 2). Thus, the transition event appears to be relatively smooth over time and the dramatic sea level drop in late March seems to be merely the result of the eventual surfacing of the pycnocline. By contrast, Huyer *et al.* (1979) considered the entire spring transition to be a rapid, single wind event process, but they concur in that the sea level drop was steric in character. A second aspect of the critical event idea is that it should be locally wind driven. Our observations give hints that this is not strictly the case. Specifically, the isopycnal surfaces began to subside around 10 April, well before the winds (Fig. 2) began to slacken. Second, the upwelling front apparently began to return to shore, and the coastal sea level began to rise (Fig. 7) before the winds began to weaken. These observations are both inconsistent with a simple, locally wind-driven interpretation. We tentatively conclude that the spring transition cannot be entirely rationalized in light of simple, locally-forced coastal upwelling.

If the spring transition event is not locally wind driven, we might then ask about its actual cause. One hypothesis would be that it represents the effects of coastal winds at lower latitude and that the resulting signal propagates poleward to Point Conception as a free coastal-trapped wave. If this were true, then presumably the spring transition sea level drop should occur sequentially at Santa Monica, Rincon Island and then at Port San Luis. As noted above, this is not the case, although it is conceivable that the offshore islands of the Southern California Bight could somehow perturb the wave propagation so as to allow such apparently anomalous propagation. A second hypothesis would be that the spring transition is somehow related to the wind stress curl or to effects having much larger offshore scales. Chelton *et al.* (1982), for example, demonstrate that dynamic height patterns having large offshore scales (200–300 km) are very closely related to very low-frequency fluctuations in coastal sea level. The offshore scales of the Chelton *et al.* (1982) pattern appear too large to be described by simple coastal-trapped waves, but otherwise, the dynamics of these fluctuations is not well understood. It may be that the spring transition is related to their dynamic height pattern, but much would remain to be explained.

The spatial structure of the Arguello–Conception upwelling system proved to be fairly complex. The mean aircraft SST (Fig. 8) shows the general structure that we had anticipated—warm water offshore and colder water close to shore, especially near (but not at) Point Arguello. Further, there is some suggestion, especially from satellite images, e.g., the figures of Bernstein *et al.* (1977) for a southward advection of colder water into the region from the coastal area to the north. Somewhat surprisingly, because the winds are often weaker there, the observed surface temperatures were also relatively cool in the Santa Barbara Channel. Otherwise, this mean pattern was more or less to be anticipated, although the upwelling center east of Point Arguello was relatively weak compared to that off Peru near 15°S.

A more novel aspect of the spatial structure is the general presence of the structures on scales of 5–15 km in observed SST. There is some suggestion (21 March) that the SST patches may represent deeper eddies, but no firm conclusions can be drawn from just one realization. In other upwelling regions, such as that off Oregon (e.g., Curtin, 1979), sea surface temperature patterns tend to be well organized during active upwelling, but patches having comparable sizes (Holladay and O'Brien, 1975) develop during wind relaxation. Curtin (1979) reports that such SST patches

off Oregon appear to be relatively superficial features confined to the upper 10–25 m of the water column. For our region, the patches are present at all observation times regardless of the wind strength and they may well penetrate to substantial depth. The generation mechanism, lifetime and translation speeds of these hypothesized eddies are unknown to us. Traditional baroclinic instability (e.g., Pedlosky, 1979, pp. 423–504) appears to be an unlikely mechanism because of the strongly stabilizing influence of the continental slope. This does not, however, appear to preclude some form of instability as a generating mechanism.

6. Conclusions

While the OPUS pilot program confirmed the presence of coastal upwelling near Points Arguello and Conception, more questions seem to have been raised than answered. However, some clear observations did result, specifically:

1) The surface wind field within the Arguello–Conception region showed substantial spatial structure, both as measured directly by anemometer and as inferred from 152 m aircraft wind measurements.

2) A spring transition-type event was observed in sea level, buoy surface temperature and in the hydrography. The event, highlighted by an abrupt drop in sea level, actually appeared to represent a more gradual oceanographic process of unknown origin.

3) The region may be the site of energetic and persistent eddy features on a scale of ~5–15 km. At the very least, the sea surface temperature fields show a good deal more dominance by structure on this scale than do other coastal upwelling regions such as that off Oregon (e.g., Curtin, 1979).

Acknowledgments. Discussions with Drs. A. J. Clarke and A. Huyer proved very helpful. R. Limeburner provided valuable assistance in the processing of the CTD data. This work was supported by National Science Foundation (NSF) Grants OCE80-21028 and OCE80-21029.

REFERENCES

Bernstein, R. L., L. Breaker and R. Whritner, 1977: California Current eddy formation: ship, air and satellite results. *Science,* **195,** 353–359.

Boyd, C. M., and S. L. Smith, 1983: Plankton, upwelling and coastally trapped waves off Peru. *Deep-Sea Res.,* **30,** 723–742.

Breaker, L. C., and R. P. Gilliland, 1981: A satellite sequence on upwelling along the California coast. *Coastal Upwelling,* F. A. Richards, Ed., *Coastal and Estuarine Sciences,* **1,** Amer. Geophys. Union, 87–94.

Brink, K. H., D. Halpern and R. L. Smith, 1980: Circulation in the Peruvian upwelling system near 15°S. *J. Geophys. Res.,* **85,** 4036–4048.

——, B. H. Jones, J. C. Van Leer, C. N. K. Mooers, D. W. Stuart, M. R. Stevenson, R. C. Dugdale and G. W. Heburn, 1981: Physical and biological structure and variability in an upwelling center off Peru near 15°S during March, 1977. *Coastal Upwelling,* F. A. Richards, Ed., *Coastal and Estuarine Sciences,* **1,** Amer. Geophys. Union, 473–495.

Chelton, D. B., P. A. Bernal and J. A. McGowan, 1982: Large-scale interannual physical and biological interaction in the California Current. *J. Mar. Res.,* **40,** 1095–1125.

Curtin, T. B., 1979: Physical dynamics of the coastal upwelling frontal zone off Oregon. Ph.D. dissertation, University of Miami, 317 pp.

Hickey, B. M., 1979: The California Current system—hypotheses and facts. *Progress in Oceanography,* Vol. 8, Pergamon, 191–279.

Holladay, C. G., and J. J. O'Brien, 1975: Mesoscale variability of sea surface temperatures. *J. Phys. Oceanogr.,* **5,** 761–772.

Huyer, A., 1980: The offshore structure and subsurface expression of sea level off Peru, 1976–1977. *J. Phys. Oceanogr.,* **10,** 1755–1768.

——, E. J. C. Sobey and R. L. Smith, 1979: The spring transition in currents over the Oregon Continental shelf. *J. Geophys. Res.,* **84,** 6995–7011.

Jones, B. H., K. H. Brink, R. C. Dugdale, D. W. Stuart, J. C. Van Leer, D. Blasco and J. C. Kelley, 1983: Observations of a persistent upwelling center off Point Conception, California. *Coastal Upwelling: Pt. A,* E. Suess and J. Thiede, Eds., Plenum, 37–60.

Kundu, P. K., and J. S. Allen, 1976: Some three-dimensional characteristics of low-frequency current fluctuations near the Oregon coast. *J. Phys. Oceanogr.,* **6,** 181–199.

Large, W. G., and S. Pond, 1981: Open ocean momentum flux measurements in moderate to strong winds. *J. Phys. Oceanogr.,* **11,** 324–336.

Limeburner, R., and R. C. Beardsley, 1979: Hydrographic station data obtained in the vicinity of Nantucket Shoals, May, July, September, 1978. Woods Hole Oceanographic Institution Tech. Rep. WHOI-79-30, 86 pp.

Pedlosky, J., 1979: *Geophysical Fluid Dynamics.* Springer-Verlag, 624 pp.

Reid, J. L., Jr., 1965: Physical oceanography of the region near Point Arguello. Tech. Rep., Inst. of Mar. Res., University of California, IMR Ref. 75-19, 30 pp.

Smith, R. L., 1974: A description of current, wind and sea level variations during coastal upwelling off the Oregon coast, July–August 1972. *J. Geophys. Res.,* **79,** 435–443.

Stuart, D. W., 1981: Sea-surface temperatures and winds during JOINT II: Part II. Temporal fluctuations. *Coastal Upwelling,* F. A. Richards, Ed., *Coastal and Estuarine Sciences,* **1,** Amer. Geophys. Union, 32–38.

——, and M. A. Linn, 1983: Meteorological and aircraft data for OPUS 1981. Florida State University Ref. FSU-MET-OPUS-83-1, 57 pp.

Sverdrup, H. V., 1938: On the process of upwelling. *J. Mar. Res.,* **2,** 155–164.